



**HAL**  
open science

# Hierarchical honeycomb material design and optimization: Beyond linearized behavior

Christelle Combescure, Ryan Elliott

► **To cite this version:**

Christelle Combescure, Ryan Elliott. Hierarchical honeycomb material design and optimization: Beyond linearized behavior. *International Journal of Solids and Structures*, 2017, 115-116, pp.161 - 169. 10.1016/j.ijsolstr.2017.03.011 . hal-01648159

**HAL Id: hal-01648159**

**<https://inria.hal.science/hal-01648159>**

Submitted on 24 Nov 2017

**HAL** is a multi-disciplinary open access archive for the deposit and dissemination of scientific research documents, whether they are published or not. The documents may come from teaching and research institutions in France or abroad, or from public or private research centers.

L'archive ouverte pluridisciplinaire **HAL**, est destinée au dépôt et à la diffusion de documents scientifiques de niveau recherche, publiés ou non, émanant des établissements d'enseignement et de recherche français ou étrangers, des laboratoires publics ou privés.



# Hierarchical honeycomb material design and optimization: Beyond linearized behavior



Christelle Combescure<sup>a,b,\*</sup>, Ryan S. Elliott<sup>a</sup>

<sup>a</sup> Department of Aerospace Engineering and Mechanics, University of Minnesota, Minneapolis, MN 55455, USA

<sup>b</sup> Laboratoire de Mécanique des Solides (CNRS UMR 7649), Ecole Polytechnique, Route de Saclay, 91128 Palaiseau, France

## ARTICLE INFO

### Article history:

Received 13 December 2016

Revised 18 February 2017

Available online 15 March 2017

### Keywords:

Stability

Bifurcation

Hierarchical honeycomb

Resilience

Non-linear material properties

Buckling

## ABSTRACT

This paper explores the importance of nonlinear material properties in the design of hierarchical honeycomb materials. The recent literature on the design and optimization of *linear* material properties for hierarchical honeycombs is reviewed. Then a full nonlinear post-bifurcation numerical analysis is performed for five representative hierarchical honeycomb structures. Particular attention is paid to the following four nonlinear material properties: the critical load  $\lambda_c$  at which the structure first experiences an instability; the plastic critical load  $\lambda_p$  at which the onset of plasticity would occur (if no elastic instability occurred); the stable post-bifurcated structure of the honeycomb; and the purely elastic resilience of the nonlinear material. It is found that although the honeycomb's linear Young's modulus is optimally maximized at a hierarchy ratio of  $\gamma_1 \approx 30\%$ , the critical load is reduced by a factor of two (relative to the standard honeycomb) at this ratio. Further, the critical load displays a monotone decreasing trend with increasing hierarchy ratio. A similar trend is found for the plastic critical load. A non-monotone trend for the resilience is discovered and explained by a qualitative change in the stable post-bifurcated structure for the hierarchical honeycombs which occurs as the hierarchy ratio is increased. The observed loss of strength (decreased critical load) is significant and may negate any advantages of the increased Young's modulus. This result demonstrates the importance of considering nonlinear properties and their implications in the design and optimization of hierarchical materials.

© 2017 Elsevier Ltd. All rights reserved.

## 1. Introduction

Hierarchy is observed in many organic materials and biological systems, as noted by Ajdari et al. (2012). It is also commonly employed in engineered systems, microstructured materials, and architectural designs (Lakes, 1993). Indeed, a self-similar hierarchical microstructure can enhance mechanical behavior and provides the opportunity to tailor a material's properties, such as mass density and Young's modulus, for its specific intended use. As a first and basic application of this principle of hierarchy, honeycomb sandwich structures have proven their efficiency and are now widely used in industry (Gibson and Ashby, 1999).

### 1.1. Design of linear material properties through hierarchy

Incorporating additional levels of hierarchy in honeycomb structures may lead to even more interesting materials. Indeed, Ajdari et al. (2012) proposed a new design that includes hierarchy

in honeycomb structures by replacing each vertex of an hexagonal honeycomb structure by a smaller hexagon (see Fig. 1). To describe the geometry of a 1st order hierarchical honeycomb structure, the ratio of the small hexagon's edge length  $b$  to the large hexagon's edge length  $a$  is defined:  $\gamma_1 \equiv b/a$ . Further, a dimensionless relative density (i.e., area fraction) is defined in terms of  $\gamma_1$  and the thickness of the cell walls (also called struts)  $t$ :  $\rho \equiv \frac{2}{\sqrt{3}}(1 + 2\gamma_1)\frac{t}{a}$ . Using an approximate analytical approach, Ajdari et al. (2012) determined the effect of  $\gamma_1$  on the hierarchical honeycomb's linearized elastic properties: Young's modulus and Poisson's ratio. They showed that the Young's modulus can be enhanced, relative to the  $\gamma_1 = 0$  standard honeycomb, by a factor of two while keeping the density  $\rho$  constant. Similarly, the Poisson's ratio can be reduced to one-third of its standard ( $\gamma_1 = 0$ ) value. These trends can be observed in Fig. 2.

As  $\gamma_1$  increases the hexagon strut thickness must decrease in order to maintain a constant density  $\rho$ . As a consequence, the aspect ratio  $t/a$  of the hexagon walls decreases, leading to an increased susceptibility to instabilities.

\* Corresponding author at: Safran Research and Technology, Rue des Jeunes Bois - Châteaufort 91128 Magny-les-Hameaux, France.

E-mail address: [christelle.combescure@polytechnique.edu](mailto:christelle.combescure@polytechnique.edu) (C. Combescure).

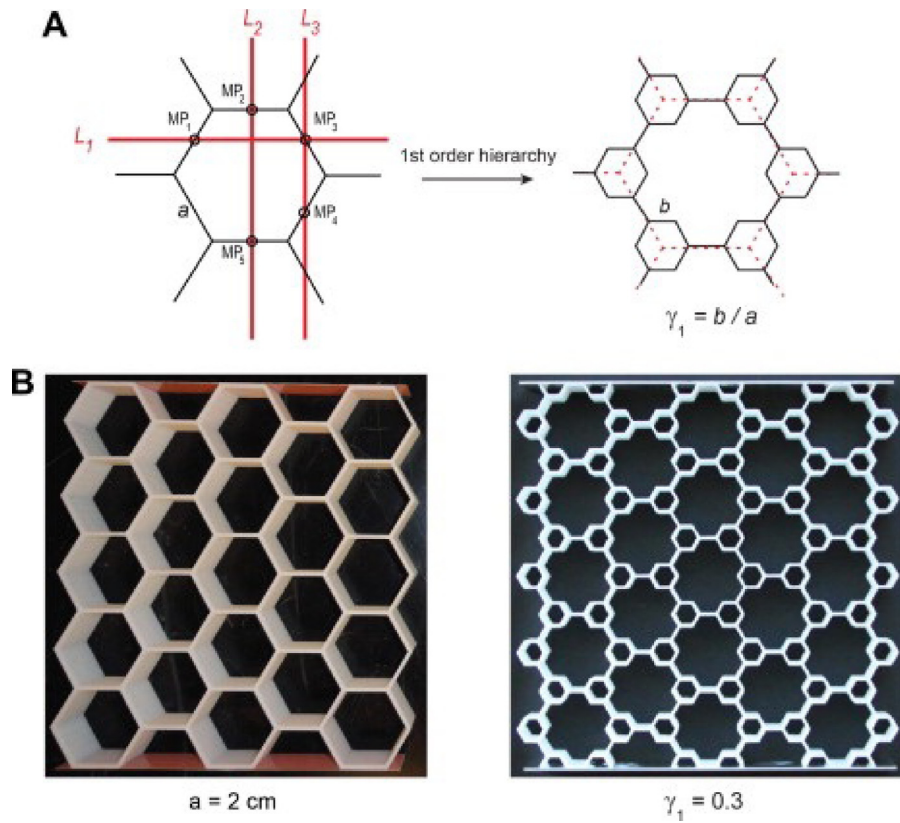


Fig. 1. Hierarchical honeycomb structures. (A) Unit cell of hierarchical honeycombs with regular structure and 1st order hierarchy. (B) Images of honeycombs fabricated using 3D printing. From Ajdari et al. (2012).

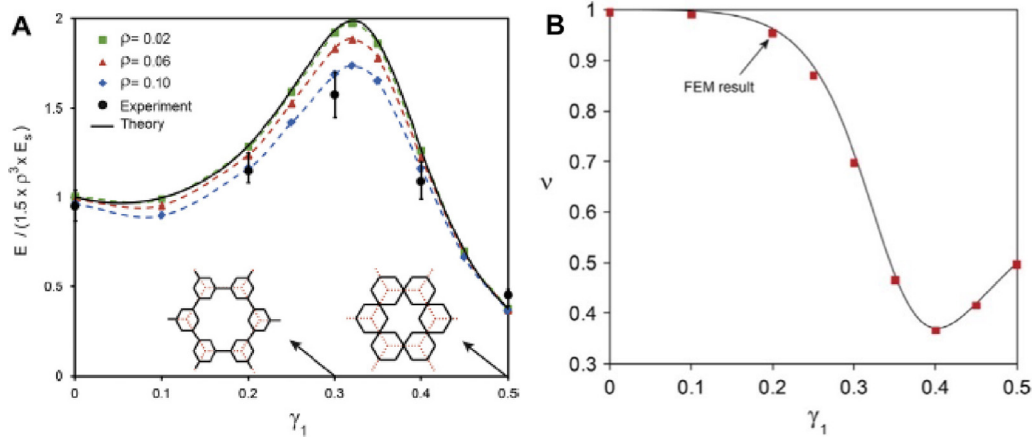


Fig. 2. (A) Normalized stiffness and for hierarchical honeycombs with 1st order hierarchy versus  $\gamma_1$ . The finite element results are shown for honeycombs with three different densities. Experimental results for structures with different  $\gamma_1$  values are also shown (black circles). (B) Poisson's ratio versus  $\gamma_1$ . From Ajdari et al. (2012).

### 1.2. Design of nonlinear material properties through hierarchy

Indeed, it is well known that standard honeycomb structures ( $\gamma_1 = 0$ ) exhibit complex nonlinear elastic bifurcation behavior when subjected to in-plane loading. For example, Combescure et al. (2016) have recently shown that when subjected to an isotropic in-plane dead-load, a honeycomb made of a linear elastic rubber-like material has an initially stiff linear response. However, upon reaching a critical load,  $\lambda_c$  (at about 12.25 kN/m, in Fig. 3) the structure undergoes a multiple bifurcation resulting in a complex post-bifurcation behavior that involves three competing equilibrium structures. This behavior is illustrated in Fig. 3 where the three bifurcating equilibrium structures (Mode I, Mode II, and

Mode III) are shown emerging, with significantly reduced stiffness (slope), from the bifurcation point on the principal loading path. As shown, the buckled equilibrium paths terminate when the hexagon struts first make contact with each other. This contact can be viewed as the onset of irreversibility in the deformation history of the honeycomb structure. Additionally in Fig. 3, the stability of the bifurcating equilibrium structures is indicated, with Mode III being the most stable structure in this case.

These results reveal a number of important nonlinear material properties. First, the critical bifurcation load  $\lambda_c$ . This material property is important because it represents the load at which the material experiences a sudden and dramatic loss of stiffness. Second, the critical plastic load  $\lambda_p$ . It is important to know if the onset of

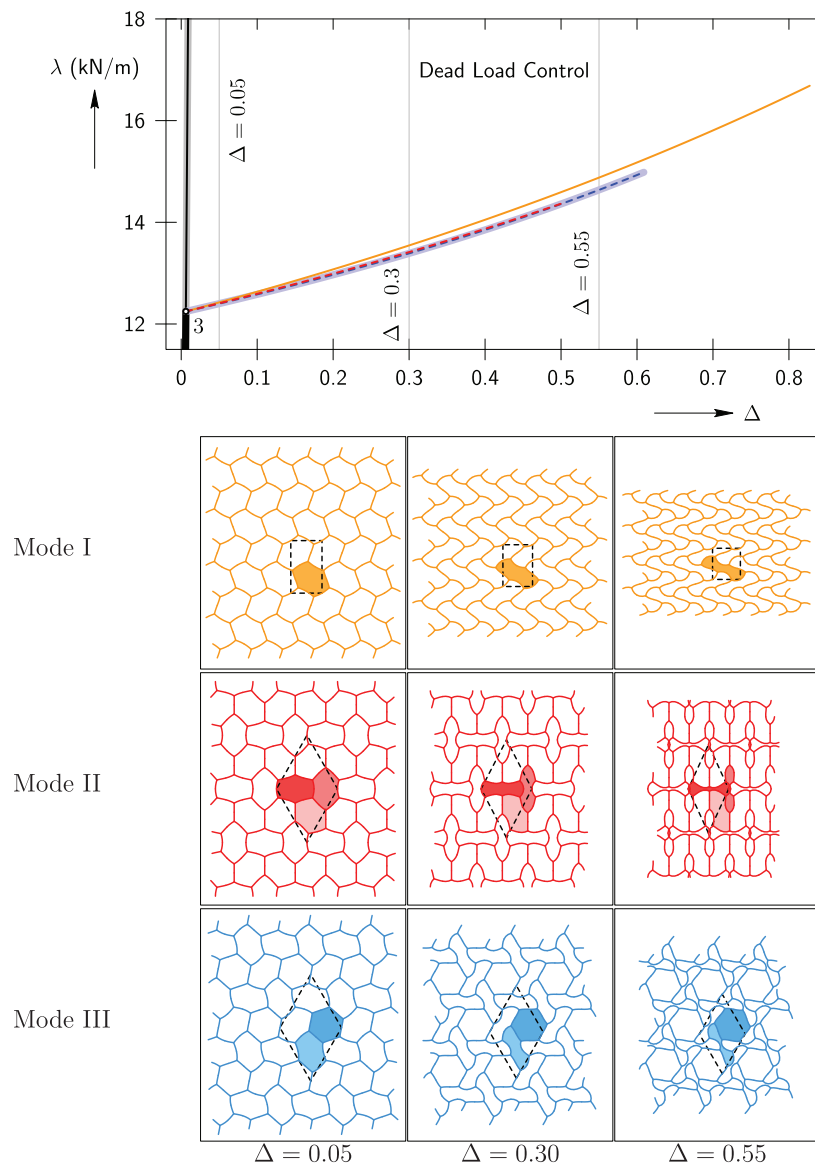


**Fig. 3.** Dead load control bifurcation diagram and deformed configurations associated with the triple Bloch-wave bifurcation of the hexagonal honeycomb structure. The diagram shows Mode I (orange), Mode II (red), and Mode III (blue) bifurcated equilibrium paths. The deformed equilibrium configuration at three loading parameters ( $\Delta = 0.05, 0.3$ , and  $0.55$ ) is shown for Mode I (first row), Mode II (second row), and Mode III (third row). Adapted from Combescure et al. (2016). (For interpretation of the references to color in this figure legend, the reader is referred to the web version of this article.)

instability for honeycomb structures occurs due to elastic buckling, as in Fig. 3, or due to plasticity. For the honeycomb material studied by Combescure et al. (2016), plasticity is initiated when the strain in a hexagon strut reaches a value of 1.52% corresponding to the average yield stress value of 35 MPa for this type of material. This corresponds to a critical plastic load of  $\lambda_p \approx 6.5\lambda_c$  that is significantly higher than the elastic critical load. Third, the stable post-bifurcated equilibrium structure for the fully elastic material. This material property can have a dramatic effect on the observed post-buckling behavior of the material. Different structures have significantly different characteristics and knowing which structure is stable predicts the properties that will be observed in practice. Finally, the elastic material's *resilience*. A material's resilience is the amount of energy that can be stored elastically and recovered upon removal of loads (Callister, 2000). For the nonlinear behavior of the standard honeycomb structure shown in Fig. 3, the material's resilience corresponds to the area under the stable portions of the unbuckled and buckled configurations. It is easy to see that a ma-

jority of the honeycomb's resilience is due to the post-bifurcation regime and that this value depends significantly on which bifurcated configuration is stable.

The design of hierarchical honeycomb materials with respect to nonlinear properties, such as those just mentioned above, is currently an active area of research and is the main area of interest in this paper. Existing studies along these lines have focused only on the onset of instability (elastic and/or plastic). In particular, recent studies of plastic collapse under uniaxial and biaxial stress (Haghpanah et al., 2014b, 2013) and elastic instability collapse under general biaxial stress (Haghpanah et al., 2014a) have been performed for hierarchical honeycomb structures. These studies derive approximate results in analytical closed form (validated by numerical results) that provide a complete map of the onset of plasticity  $\lambda_p$  as well as elastic buckling loads  $\lambda_c$  in the three-dimensional general stress space.

Although these studies are the first to look at the nonlinear onset of elastic and plastic instability of hierarchical honey-

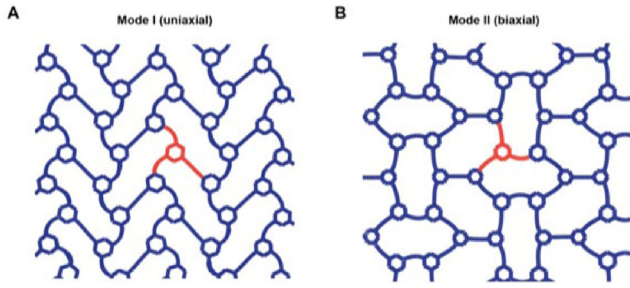


Fig. 4. Bifurcation modes (A) I and (B) II for hierarchical honeycomb structures identified from finite element simulations. From Haghpanah et al. (2014a).

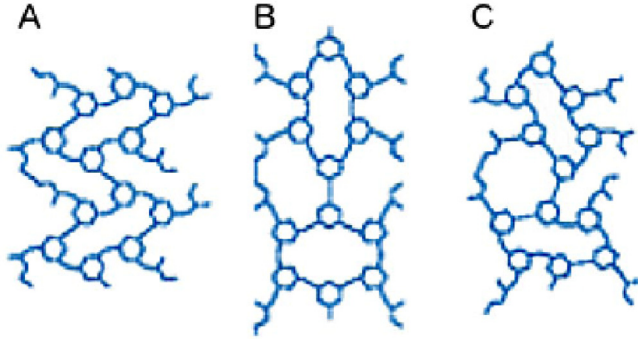


Fig. 5. Bifurcation modes (A) I, (B) II and (C) III for hierarchical honeycomb structures identified from finite element simulations. From Mousanezhad et al. (2015b).

comb materials, their methods introduce a number of significant approximations. For example, elastic buckling behavior was studied using analytical methods based on the beam-column solution (Timoshenko and Gere, 2009). In order for such an analytical study to be possible, the authors' had to introduce *predefined and fixed buckling modes* (motivated by either the results of finite element simulations or buckling modes found in the existing literature). Only then is it possible to develop closed-form relations for the buckling strength of the hierarchical honeycombs. In particular, it was assumed that the small hexagons of the hierarchical honeycomb structure deform as rigid bodies. This assumption results in a significant restriction of the range of  $\gamma_1$  for which their results can be considered valid. Moreover, only two bifurcation modes were identified from the finite element computations (see Fig. 4), whereas Mousanezhad et al. (2015b) identified three modes, similar to the three modes of standard hexagonal honeycomb structures (see Figs. 3 and 5).

In order to more fully investigate these nonlinear material properties and to look, for the first time, at the stable post-bifurcated equilibrium structure and the resilience of hierarchical honeycomb structures, the present study uses a predictive method based on group representation theory (Healey, 1988; Zingoni, 2002; Saiki et al., 2005; Okumura et al., 2002) and branch-following and bifurcation techniques (Elliott et al., 2002; Elliott, 2007) to determine how these nonlinear properties vary over the whole range of  $\gamma_1$  for equibiaxial dead-load conditions. One aim of this study is to complement the results presented in Mousanezhad et al. (2015a), who study the influence of hierarchy ratio on the stable bifurcated modes and Poisson's ratio of hierarchical honeycombs subjected to uniaxial compression. In particular, Mousanezhad et al. (2015a) show that, under uniaxial compression along either the  $x$  or  $y$  axes, the stable bifurcation mode changes when the hierarchy ratio exceeds 37.5%.

In the remainder of this paper, we briefly describe the modeling and simulation techniques used in Section 2. These methods provide accurate load–deformation paths and rigorously characterize

the stability of each (unbuckled and buckled) honeycomb equilibrium configuration. We then present, in Section 3, detailed results for the behavior of five hierarchical honeycomb structures with values of  $\gamma_1$  spanning the entire physically relevant range. From these results, we highlight the variation of four nonlinear material properties: the critical bifurcation load  $\lambda_c$ , the critical plastic load  $\lambda_p$ , the stable post-bifurcated equilibrium structure, and the resilience.

## 2. Methods and material constitutive parameters

We follow the approach recently developed in Combescure et al. (2016), where the finite element method (FEM) code FEAP (Taylor, 1987) is used to discretize the honeycomb hexagon struts using two-dimensional large displacement large rotation frame elements with shear deformation. Thus, hexagon vertices (where three struts join) are modeled as rigid welded joints such that the angle at the joint between any two struts is always  $120^\circ$ . However, during loading, a joint may deform as a rigid-body. That is, it may translate in two-dimensions and rotate about the out-of-plane axis. The FEAP frame elements are coupled with a linear elastic material constitutive law using parameter values of  $E = 2.3$  GPa,  $\nu = 0.3$  for Young's modulus and Poisson's ratio, respectively. In order to investigate the onset of plasticity along the primary equilibrium path, a criterion on the plastic yield strain is set up at  $\epsilon_p = 0.0152$ . A reference strut length of  $a = 2.0$  cm and thickness of  $t = 0.175$  cm provide a reference relative density of  $\rho = 0.101$  for the standard ( $\gamma_1 = 0$ ) honeycomb structure. These values are consistent with those used by Ajdari et al. (2012) in their study of hierarchical honeycomb structures.

As in Combescure et al. (2016), the FEM code is coupled with a custom computational code that implements uniform deformation with periodic displacement oscillations (i.e., *Lagrangian Cauchy–Born Kinematics*) of a hierarchical honeycomb unit cell to obtain the honeycomb material's effective strain energy (per unit cell)  $W(\mathbf{U}, \hat{\mathbf{v}})$ , where  $\mathbf{U}$  is the symmetric right-stretch tensor describing the material's uniform deformation and  $\hat{\mathbf{v}}$  is a vector of degrees-of-freedom (DOFs) representing the periodic displacement oscillations corresponding to the FEM mesh nodal DOFs. The custom code also implements a two-dimensional far-field isotropic dead-loading device such that the total energy (per unit cell) for the infinite perfect hierarchical honeycomb material is given by

$$\hat{\mathcal{E}}(\mathbf{q}; \lambda) = \hat{\mathcal{E}}(\mathbf{U}, \hat{\mathbf{v}}; \lambda) \equiv W(\mathbf{U}, \hat{\mathbf{v}}) + \lambda \operatorname{tr}(\mathbf{U} - \mathbf{I})A_{\text{cell}}, \quad (1)$$

where  $\mathbf{q} \equiv (\mathbf{U}, \hat{\mathbf{v}})$  is an array containing the complete set of DOFs,  $\lambda$  is the scalar loading amplitude,  $\mathbf{I}$  is the two-dimensional second-order identity tensor, and  $A_{\text{cell}}$  is the reference area of a primitive hierarchical honeycomb unit cell. The deformation parameter associated with  $\lambda$  is  $\Delta = \operatorname{tr}(\mathbf{I} - \mathbf{U})$  which represents the compressive Biot strain.

The hierarchical honeycomb material's equilibrium configurations as a function of the loading are then given by the derivative of its energy

$$\frac{\partial \hat{\mathcal{E}}}{\partial \mathbf{q}} = \begin{bmatrix} \frac{\partial \hat{\mathcal{E}}}{\partial \mathbf{U}} \\ \frac{\partial \hat{\mathcal{E}}}{\partial \hat{\mathbf{v}}} \end{bmatrix} = \mathbf{0}. \quad (2)$$

These equations are solved using branch-following and bifurcation methods (as described in Combescure et al., 2016) to obtain bifurcation diagrams such as the one shown in Fig. 3.

In addition to the generation of bifurcation diagrams, the custom numerical code performs a detailed and rigorous stability analysis of each equilibrium configuration. This includes evaluation of the *rank-one convexity* condition as well as the *Bloch wave stability* condition. Together, these two criteria provide rigorous neces-

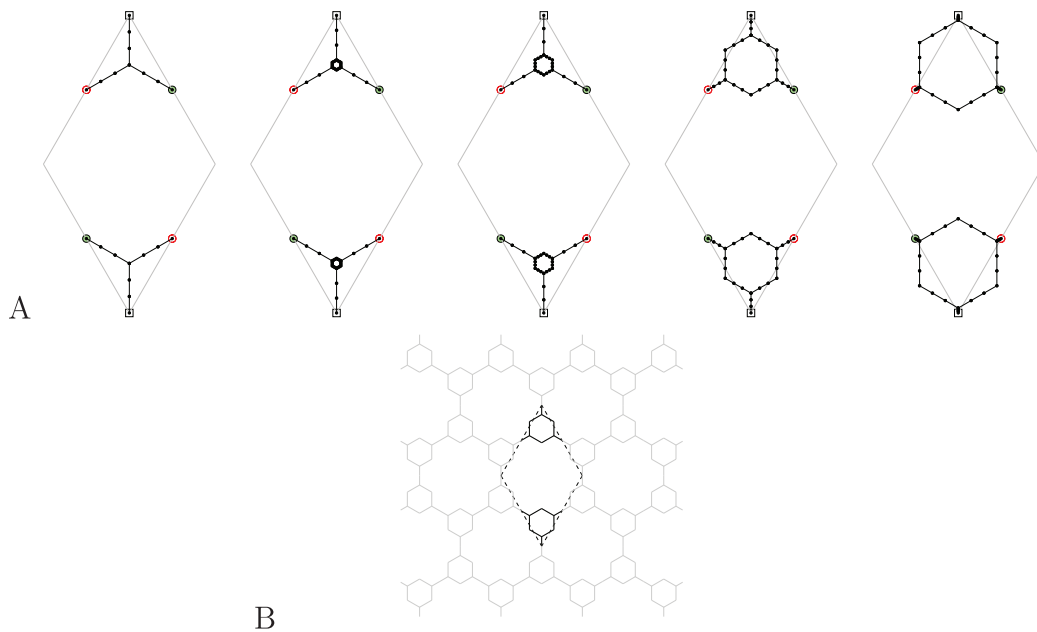


**Fig. 6.** A. Finite element meshes for the  $1 \times 1$  cell of hierarchical honeycombs with  $\gamma_1 = 0\%$  (classical), 5%, 10%, 30% and 45%, from left to right. Similar symbols on boundary nodes indicate pairs of periodic boundary nodes. B. Example of periodic arrangement of hierarchical honeycombs with  $\gamma_1 = 30\%$ . The  $1 \times 1$  cell is represented in black surrounded by dashed lines.

sary conditions for the equilibrium configuration to be stable (with respect to all bounded perturbations) in the Lyapunov sense.

### 3. Results and discussion

In this section, we present results for five representative hierarchical honeycomb structures with values of  $\gamma_1 = 0\%$ , 5%, 10%, 30%, and 45%, holding the density at<sup>1</sup>  $\rho = 0.101$ . We selected  $\gamma_1 = 0\%$  since this corresponds to the well known honeycomb structure. The values of  $\gamma_1 = 5\%$  and 10% represent small and medium perturbations of the standard honeycomb structure. According to the results of [Ajdari et al. \(2012\)](#) a value of  $\gamma_1 = 30\%$  provides a nearly optimal Young's modulus for the hierarchical honeycomb structure. Finally,  $\gamma_1 = 45\%$  represents a structure approaching the upper limit of  $\gamma_1 = 50\%$ , where the entire hexagon strut of length  $a$  is replaced by two hexagons of side length  $a/2$ .

[Fig. 6](#) shows the FEM meshes<sup>2</sup> we used for the ( $1 \times 1$  unit cell) principal equilibrium path computations. As discussed in [Combescure et al. \(2016\)](#), periodic boundary conditions on displacements and rotations are applied to corresponding pairs of boundary nodes (shown with similar symbols in [Fig. 6](#)). A mesh convergence study (not presented here) determined that meshes with 3 elements per hierarchical hexagon strut provide sufficient precision with acceptable computational expense.

#### 3.1. $\gamma_1 = 0\%$ – standard honeycomb structure

Consistent with the results of [Combescure et al. \(2016\)](#) shown in [Fig. 3](#), the classical honeycomb structure subjected to equibiaxial compressive loading has a linear load versus deformation principal equilibrium path as shown in [Fig. 7](#). The Cascading-Cauchy-Born algorithm ([Sorkin et al., 2014](#)) identifies a  $2 \times 2$  unit cell that must be used to compute the bifurcating equilibrium

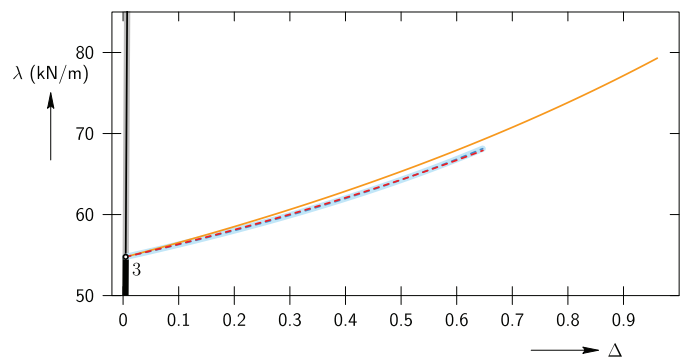


**Fig. 7.** Bifurcation diagram for the hierarchical honeycomb with  $\gamma_1 = 0\%$ . The principal equilibrium path is stable (solid line segment) for  $\lambda < \lambda_c \approx 55$  kN/m and unstable (dashed line segment) for larger load values. At the critical load  $\lambda_c$  three energetically distinct equilibrium paths bifurcate from the principal path. An open circle labeled with a number on the path corresponds to a Hessian bifurcation point and indicates the number of eigenvalues that become zero simultaneously.

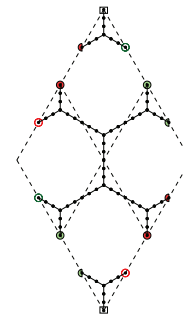


**Fig. 8.** Finite element mesh for the  $2 \times 2$  honeycomb unit cell. Similar symbols on boundary nodes indicate periodic boundary nodes.

<sup>1</sup> For constant density, the strut thickness ratio follows the relation  $t/a = (1 + 2\gamma_1)t_0/a$ , where  $t_0/a = 0.0875$  is the thickness for zero hierarchy.

<sup>2</sup> Even though, for the cases of  $\gamma_1 = 30\%$  and 45%, the small hexagon nodes fall outside the unit cell outline, all nodes and finite elements shown can be unambiguously assigned to a single unit cell.

paths for the honeycomb structure. This unit cell is shown in [Fig. 8](#). The identification of the  $2 \times 2$  unit cell is based on the unstable wave-vectors resulting from a Bloch-wave stability analysis on the principal equilibrium path. Along the principal equilibrium path,

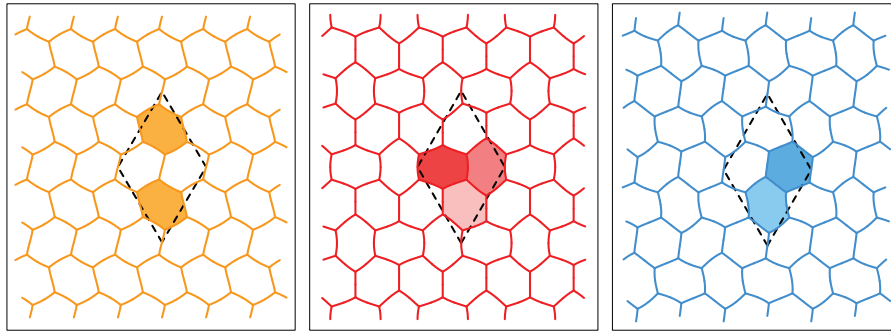


**Fig. 9.** Deformation modes at the first triple bifurcation point of the  $\gamma_1 = 0\%$  standard honeycomb structure. The modes are labeled I (yellow), II (red), and III (blue) from left to right, respectively. (For interpretation of the references to color in this figure legend, the reader is referred to the web version of this article.)

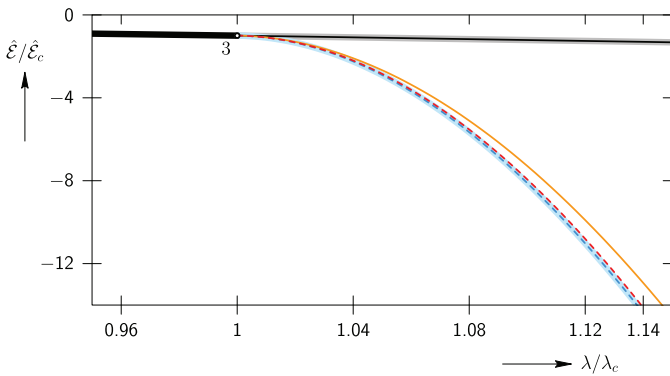


**Fig. 10.** Normalized total energy versus loading parameter  $\lambda$  for the  $\gamma_1 = 0$  honeycomb. The principal equilibrium path and three bifurcating paths are shown. Heavy solid line segments indicate stability with respect to both RK1, Bloch-wave, and ad-hoc stable. Thin solid line segments indicate equilibrium configurations that are RK1 stable but Bloch wave and ad-hoc unstable. Dashed line segments with a light background indicate equilibrium configurations that are stable only with respect to the ad-hoc criterion. Finally, dashed line segments are unstable with respect to all stability criteria considered in this work. Open circles with numbers on the paths correspond to Hessian bifurcation points and indicate the number of eigenvalues that become zero simultaneously.

the first bifurcation point corresponds to a triple bifurcation and three bifurcation modes are identified (see Fig. 9). Associated with each of these modes is a set of symmetry-related bifurcating equilibrium paths that emerge from the bifurcation point at  $\lambda_c$ . Powerful branch-following and bifurcation techniques allow us to follow the bifurcated branches. Then the stability of these branches as well as their total energy can be determined. The stable branch with minimal total energy should be the one followed by the real system. Fig. 10 plots the total energy  $\hat{E}$  versus the loading parameter  $\lambda$  normalized by their values ( $\hat{E}_c$  and  $\lambda_c$ , respectively) at the critical point and shows that the stable minimal energy path is the one corresponding to Mode III. These results coincide with the theoretical and experimental results presented by Papka and Kyriakides (1999); Okumura et al. (2002). The determination of an equilibrium configuration's stability is a subtle issue. As discussed in depth by Combescure et al. (2016), two necessary stability criteria may be employed. These are the Bloch-wave and rank-one convexity (RK1) criteria. The Bloch-wave criterion provides necessary conditions for the equilibrium configuration to be stable with respect to arbitrary bounded perturbations, whereas the rank-one stability criterion provides necessary conditions for the configuration to be stable with respect to long wavelength (shear-strain-like) perturbations. Together, these two criteria provide a rigorous set of necessary conditions that a material equilibrium configuration must satisfy in order to be stable. In addition to these two

criteria, Combescure et al. (2016) identify a third criterion: the *ad-hoc* criterion, which corresponds to local minimization of the material's total energy density function. This criterion, although commonly employed, is not strictly necessary nor sufficient to guarantee stability of the equilibrium configuration. However, due to the common use of the ad-hoc criterion, it is included to highlight the differences between it and the rigorous Bloch-wave and RK1 criteria.

In Figs. 7 and 10, Heavy solid line segments indicate stability with respect to the RK1, Bloch-wave, and ad-hoc criteria. Thin solid line segments indicate equilibrium configurations that are RK1 stable but Bloch wave and ad-hoc unstable. Dashed line segments with a light background indicate equilibrium configurations that are stable only with respect to the ad-hoc criterion. Finally, dashed line segments are unstable with respect to all stability criteria considered in this work. In the  $\gamma_1 = 0\%$  case, we see from Fig. 10 that the lowest energy path is the Mode III (also referred to as the “flower mode”) bifurcated equilibrium configuration. However, none of the three modes satisfy the two necessary stability criteria. Thus, the stable post bifurcated equilibrium configuration is, strictly, not identified by the presented results. Instead, it is likely that the stable structure is another bifurcated equilibrium path similar to the flower mode but exhibiting fluctuations with a long wavelength periodicity. Despite this, we will identify the Mode III equilibrium configuration as representative of the physically relevant post-bifurcation behavior of the  $\gamma_1 = 0\%$  honeycomb structure. Luckily, as we will soon see, this complication disappears for the  $\gamma_1 > 0\%$  hierarchical honeycomb structures.

From the results of Figs. 7 and 10 we can, again, observe the nonlinear material properties of interest for this work. The critical load  $\lambda_c$  is immediately apparent. The critical plastic load  $\lambda_p \approx 6.5\lambda_c$  on the principal path is off-scale in Fig. 7. The stable post-bifurcated equilibrium structure has been associated with the Mode III path. And, finally, the resilience of the purely elastic material is the area under the stable principal path segment and the Mode III curve in Fig. 7. However, note that if plasticity is considered for the bifurcated equilibrium paths, then it is found that the onset of plasticity occurs soon after the bifurcation point at  $\lambda_{p2} \approx 1.003\lambda_c$ . This is in good agreement with results presented in Okumura et al. (2004).

Now that we have reviewed our computational method and discussed in depth the results for the  $\gamma_1 = 0\%$  case, we will present results for the remaining cases and draw conclusions.

### 3.2. $\gamma_1 > 0\%$ – hierarchical honeycomb structures

Simulations similar to the one described for the  $\gamma_1 = 0\%$  honeycomb in the previous section were performed for each of the remaining four honeycomb configurations. The results are similar to

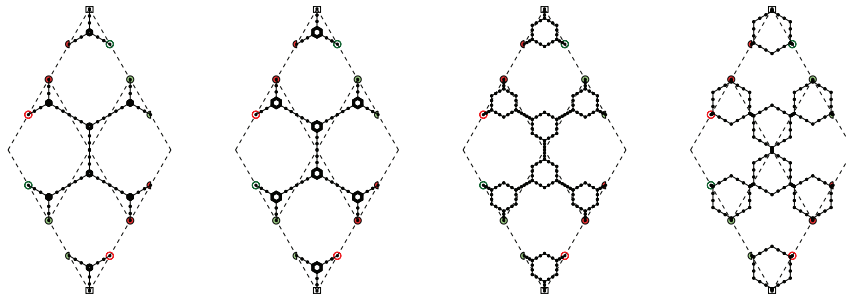


**Fig. 11.** Finite element mesh for the  $2 \times 2$  unit cells with hierarchical ratio  $\gamma_1$  equal to 5%, 10%, 30% and 45%, from left to right. Similar symbols on boundary nodes have periodic boundary conditions applied.

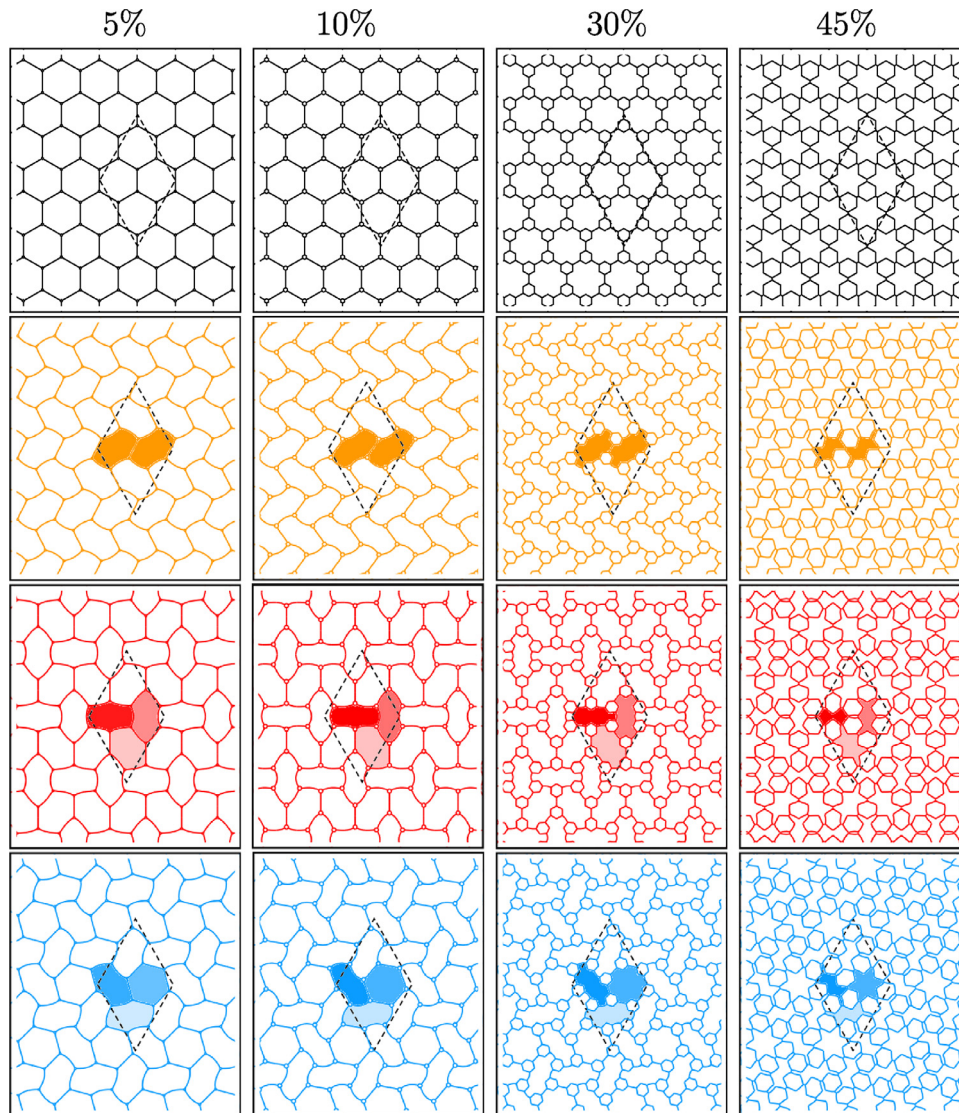


**Fig. 12.** Undeformed configuration (black) and deformation modes I (yellow), II (red), and III (blue) at the first triple bifurcation point of the hierarchical honeycomb structures with  $\gamma_1$  equal to 5%, 10%, 30% and 45%, from left to right. (For interpretation of the references to color in this figure legend, the reader is referred to the web version of this article.)

those found for the standard honeycomb case. However, there are quantitative differences and one significant qualitative change. In particular, as the hierarchical ratio  $\gamma_1$  increases the Mode I structure becomes stable with respect to both the Bloch-wave and RK1 criteria. Further, it becomes the minimum energy configuration. These changes and their effects on the hierarchical honeycomb's nonlinear material properties are explained further below.

**Bifurcation modes.** In all of the studied hierarchical honeycomb structures the first bifurcation is a triple bifurcation related to a Bloch-wave instability which requires a  $2 \times 2$  honeycomb unit cell in order to simulate the post-bifurcation behavior. The necessary unit cells for the  $\gamma_1 = 5, 10, 30, 45\%$  honeycombs are shown in Fig. 11. At the bifurcation point for each value of  $\gamma_1$ , three bifurcation modes are identified and are presented in Fig. 12. These

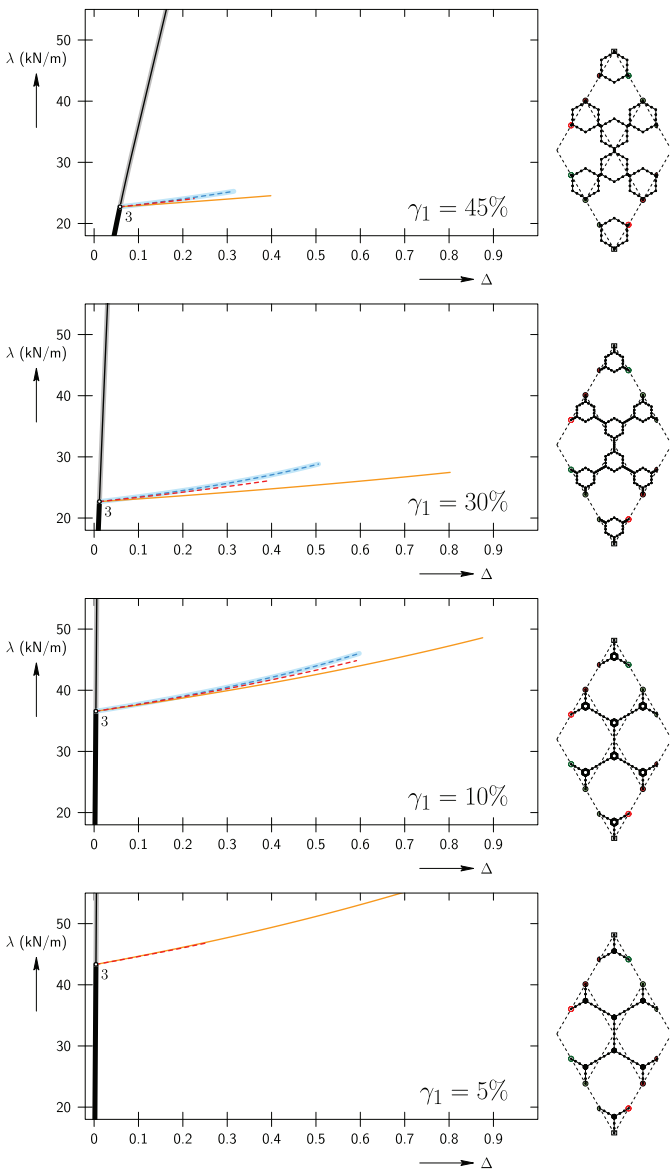


**Fig. 13.** Post-bifurcation behavior of hierarchical honeycomb structures with  $\gamma_1 = 5, 10, 30,$  and  $45\%$ . Clear trends in the nonlinear properties are observed. The critical load  $\lambda_c$  decreases as  $\gamma_1$  increases; the stable post-bifurcated equilibrium structure is Mode III for very small values of  $\gamma_1$ , but quickly switches to Mode I as  $\gamma_1$  increases away from zero; and the resilience is seen to have a jump increase, followed by a smooth decrease as  $\gamma_1$  increases.

modes are very similar to those identified for  $\gamma_1 = 0\%$ . Note that for the  $\gamma_1 = 30\%$  and  $45\%$  honeycombs the smaller hexagons undergo deformation whereas they behave essentially as rigid structures for smaller values of  $\gamma_1$ . This provides evidence for the hypothesis of Haghpanah et al. (2014a), where the small hexagons were assumed rigid. However, we find that this assumption is not valid for larger values of  $\gamma_1$ . Further, our results capture the existence of the “flower” Mode III for hierarchical structures; this mode was discussed by Mousanezhad et al. (2015b) but ignored by Haghpanah et al. (2014a).

**Post-bifurcation analysis.** Using the methods of Combescure et al. (2016) the post-bifurcation behavior of the hierarchical honeycomb structures is determined. These results are displayed in Fig. 13. Here we see significant changes in the nonlinear material properties of the honeycomb structures as the hierarchy ratio  $\gamma_1$  increases. In Fig. 13 it is easily observed that the critical load  $\lambda_c$

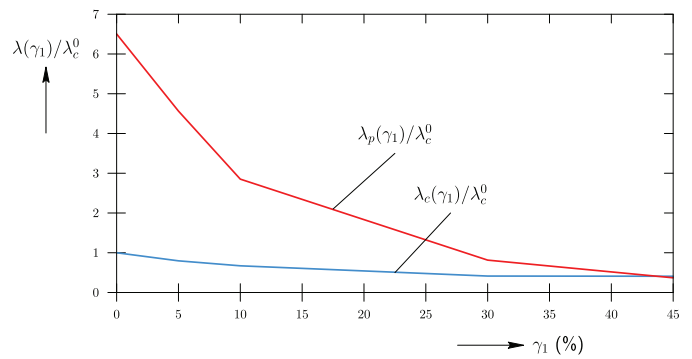


**Fig. 14.** Evolution of the elastic critical load  $\lambda_c$  (in blue) and plastic critical load  $\lambda_p$  (in red), normalized by the value of  $\lambda_c$  for  $\gamma_1 = 0\%$ . (For interpretation of the references to color in this figure legend, the reader is referred to the web version of this article.)

**Table 1**

Variation of stiffness, critical load  $\lambda_c$ , plastic critical load  $\lambda_p$  and resilience with hierarchy ratio  $\gamma_1$ , and the associated stable post-bifurcation structure.

$\gamma_1$	0%	5%	10%	30%	45%
Mode	III	III	I	I	I
Stiffness (MPa)	3.558	3.439	3.539	6.873	2.478
Critical load $\lambda_c$ (kN/m)	54.78	43.34	36.57	22.69	22.73
Plastic critical load $\lambda_p$ (kN/m)	356.2	250.0	156.2	44.61	20.26
Resilience ( $\text{J}\cdot\text{m}^{-2}$ )	36.45	28.6	37.12	19.82	8.03

decreases as  $\gamma_1$  increases. Similarly, the critical plastic load  $\lambda_p$  is initially much larger than  $\lambda_c$ , but decreases more rapidly with  $\gamma_1$  until  $\lambda_p \approx \lambda_c$  for  $\gamma_1 = 45\%$ . These trends can be seen quantitatively in Fig. 14.

One of the most interesting results of this study is the discovery that the stable post-bifurcated equilibrium structure changes, from the flower Mode III structure to the Mode I structure, after a small increase in  $\gamma_1$ . Indeed, the Mode I structure becomes the low energy stable structure once the hierarchy ratio reaches  $\gamma_1 = 10\%$ . This is confirmed by the Bloch-wave stability analysis, shown in Fig. 15, where it is observed that even for very long wavelength perturbations the Mode I structure is stable for  $\gamma_1 = 10\%$  whereas Mode III is unstable for  $\gamma_1 = 5\%$ , as previously observed in Combescure et al. (2016) for a classical honeycomb structure. Thus, introducing hierarchy in a honeycomb structure induces a change in the stable post-bifurcation mode and stabilizes it with respect to long-wavelength instabilities.

Initially, the resilience decreases as the critical load  $\lambda_c$  decreases with increasing  $\gamma_1$ . However, the qualitative transition from a Mode III stable post-bifurcated structure to Mode I, leads to a significant jump increase in the resilience. This is followed by a more smooth decrease in accord with the decreasing  $\lambda_c$  and the significantly decreasing value of  $\Delta$  corresponding to the point of first strut contact (and associated loss of reversibility). Quantitative values for the resilience are provided in Table 1.

#### 4. Discussion & conclusions

In this work a hierarchical honeycomb design is explored to understand the effects of hierarchy on linear and nonlinear material properties of the structure. The focus is on the nonlinear behavior and properties of these materials because the existence of instabilities leads to dramatic shifts in the material’s effective strength and other properties. We hope this example will serve as a reminder of the importance of considering nonlinear behavior in the process of design and optimization of materials.

We focus on four nonlinear material properties of hierarchical honeycombs: the critical load  $\lambda_c$  at which the structure first ex-

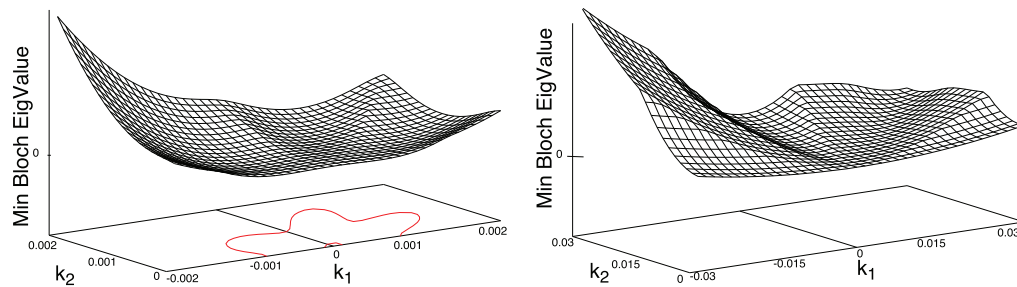


**Fig. 15.** Bloch-wave minimum eigenvalue surface near the point  $\mathbf{k} = (0, 0)$ , almost immediately after bifurcation along the Mode III path (left) for a 5% hierarchical honeycomb structure and along the Mode I path (right) for a 10% hierarchical honeycomb structure. Negative eigenvalues indicate instability. Zero eigenvalue contours are plotted in red below the eigenvalue surface. It is observed that all Bloch-wave eigenvalues are stable for the Mode I path of the 10% hierarchical structure, whereas the Mode III path of the 5% hierarchical structure has a region of instability surrounding  $\mathbf{k} = (0, 0)$ . (For interpretation of the references to color in this figure legend, the reader is referred to the web version of this article.)

periences an instability; the plastic critical load  $\lambda_p$  at which the onset of plasticity would occur (if no elastic instability occurred); the stable post-bifurcated structure of the honeycomb; and the resilience of the purely elastic nonlinear material. Although the nonlinear investigation of such structures is significantly more complicated than a linear analysis, our recent developments for such analyses (Combescure et al., 2016) make this a relatively straight forward task.

From our analysis, we find that the critical load  $\lambda_c$  significantly decreases as the hierarchy ratio  $\gamma_1$  increases. This trend is opposite to that of the linear Young's modulus, which increases with  $\gamma_1$  until a maximum is reached around  $\gamma_1 = 30\%$ . By comparing Figs. 2 and 14, it can be seen that although optimization can achieve a factor of two increase in stiffness, this is intrinsically accompanied by a reduction, by a factor of two, in the material's strength (critical load). This significant reduction in strength may very well negate any practical gains associated with the increased stiffness. This is a potent example of the care that must be taken when designing optimized materials.

In addition to the significant decrease in critical load with increasing hierarchy, we also identify a dependence of the stable post-bifurcated structure on the hierarchy ratio as well as a non-monotone trend for the resilience of the honeycomb structures.

## Acknowledgments

Authors would like to thank Prof. Nicolas Triantafyllidis of the Laboratoire de Mécanique des Solides & Ecole Polytechnique, France and CNRS for his helpful suggestions, discussions, and support, as well as our reviewers for their precious comments and advice on our paper and bibliography.

This work was partially supported by: National Science Foundation (NSF) grant PHY-0941493 and grant CMMI-1462826, the Andre Citroen Chair at the Ecole Polytechnique and the Solid Mechanics Laboratory (LMS) of the Ecole Polytechnique. We also acknowledge support by the University of Minnesota Supercomputing Institute.

## References

Ajdari, A., Jahromi, B., Papadopoulos, J., Nayeb-Hashemi, H., Vaziri, A., 2012. Hierarchical honeycombs with tailorable properties. *Int. J. Solids Struct.* 49, 1413–1419.

- Callister Jr., W.D., 2000. *Materials Science and Engineering: An Introduction*, 5th John Wiley & Sons.
- Combescure, C., Henry, P., Elliott, R.S., 2016. Post-bifurcation and stability of a finitely strained hexagonal honeycomb subjected to equi-biaxial in-plane loading. *Int. J. Solids Struct.* 88, 296–318.
- Elliott, R.S., 2007. Multiscale bifurcation and stability of multilattices. *J. Comput.-Aided Mater. Des.* 14 (1), 143–157.
- Elliott, R.S., Shaw, J.A., Triantafyllidis, N., 2002. Stability of thermally-induced martensitic transformations in bi-atomic crystals. *J. Mech. Phys. Solids* 50 (11), 2463–2493.
- Gibson, L.J., Ashby, M.F., 1999. *Cellular Solids: Structure and Properties*. Cambridge University Press.
- Haghpanah, B., Oftadeh, R., Papadopoulos, J., Vaziri, A., 2013. Self-similar hierarchical honeycombs. In: *Proceedings of the Royal Society of London A: Mathematical, Physical and Engineering Sciences*, 469. The Royal Society, p. 20130022.
- Haghpanah, B., Papadopoulos, J., Mousanezhad, D., Nayeb-Hashemi, H., Vaziri, A., 2014a. Buckling of regular, chiral and hierarchical honeycombs under a general macroscopic stress state. In: *Proceedings of the Royal Society of London A: Mathematical, Physical and Engineering Sciences*, 470. The Royal Society, p. 20130856.
- Haghpanah, B., Papadopoulos, J., Vaziri, A., 2014b. Plastic collapse of lattice structures under a general stress state. *Mech. Mater.* 68, 267–274.
- Healey, T.J., 1988. A group-theoretic approach to computational bifurcation problems with symmetry. *Comput. Methods Appl. Mech. Eng.* 67 (3), 257–295.
- Lakes, R., 1993. Materials with structural hierarchy. *Nature* 361, 511–515.
- Mousanezhad, D., Babae, S., Ebrahimi, H., Ghosh, R., Hamouda, A.S., Bertoldi, K., Vaziri, A., 2015a. Hierarchical honeycomb auxetic metamaterials. *Sci. Rep.* 5.
- Mousanezhad, D., Babae, S., Ghosh, R., Mahdi, E., Bertoldi, K., Vaziri, A., 2015b. Honeycomb phononic crystals with self-similar hierarchy. *Phys. Rev. B* 92 (10), 104304.
- Okumura, D., Ohno, N., Noguchi, H., 2002. Post-buckling analysis of elastic honeycombs subject to in-plane biaxial compression. *Int. J. Solids Struct.* 39 (13), 3487–3503.
- Okumura, D., Ohno, N., Noguchi, H., 2004. Elastoplastic microscopic bifurcation and post-bifurcation behavior of periodic cellular solids. *J. Mech. Phys. Solids* 52 (3), 641–666.
- Papka, S., Kyriakides, S., 1999. Biaxial crushing of honeycombs:—part 1: experiments. *Int. J. Solids Struct.* 36 (29), 4367–4396.
- Saiki, I., Ikeda, K., Murota, K., 2005. Flower patterns appearing on a honeycomb structure and their bifurcation mechanism. *Int. J. Bifurcation Chaos* 15 (02), 497–515.
- Sorkin, V., Elliott, R.S., Tadmor, E.B., 2014. A local quasicontinuum method for 3d multilattice crystalline materials: application to shape-memory alloys. *Modell. Simul. Mater. Sci. Eng.* 22 (5), 055001.
- Taylor, R.L., 1987. *FEAP-ein Finite Element Analysis Programm*. Ing.-Gemeinschaft Klee & Wrigges.
- Timoshenko, S.P., Gere, J.M., 2009. *Theory of Elastic Stability*. Courier Corporation.
- Zingoni, A., 2002. Group-theoretic applications in solid and structural mechanics: a review. In: *Computational Structures Technology*. Civil-Comp press, pp. 283–317.